

***Final Draft***  
**of the original manuscript:**

Winterfeldt, J.; Geyer, B.; Weisse, R.:

**Using QuikSCAT in the added value assessment of dynamically  
downscaled wind speed**

In: International Journal of Climatology (2010) Wiley

DOI: 10.1002/joc.2105

# Using QuikSCAT in the added value assessment of dynamically downscaled wind speed

JÖRG WINTERFELDT \*

GKSS, INSTITUTE FOR COASTAL RESEARCH, GEESTHACHT, GERMANY

BEATE GEYER

GKSS, INSTITUTE FOR COASTAL RESEARCH, GEESTHACHT, GERMANY

RALF WEISSE

GKSS, INSTITUTE FOR COASTAL RESEARCH, GEESTHACHT, GERMANY

---

\* *Corresponding author address:* Jörg Winterfeldt, GKSS Research Center, Institute for Coastal Research, Max-Planck-Straße 1, 21502 Geesthacht, Germany.  
Current affiliation: GE Wind Energy, 48499 Salzbergen, Germany.  
E-Mail: j\_winterfeldt@hotmail.com

## ABSTRACT

Hindcasts with reanalysis driven regional climate models (RCMs) are a common tool to assess weather statistics (i.e. climate) and recent changes and trends. A remote sensing based method to investigate the added value of surface marine RCM wind speed is introduced: The capability of the dynamical downscaling approach (with spectral nudging applied) to add value to the reanalysis wind speed forcing is assessed by the comparison with QuikSCAT Level 2B 12.5 km (L2B12) swath data in European waters for 2000 to 2007. Co-location criteria are within  $0.1^\circ$  and  $0.06^\circ$  in longitudinal and latitudinal distance from RCM grid points and within 10 minutes. In the wind speed range QuikSCAT L2B12 is reliably reproducing ( $3\text{-}20\text{ m s}^{-1}$ ), dynamically downscaled wind speed does not show an added value in “open ocean“ areas. However in coastal areas with complex topography the regional models show an added value, especially around Iceland and the Iberian peninsula and in the Mediterranean, Baltic and Irish Seas, validating the findings of previous in-situ data based studies on the added value. Strong inter-seasonal differences exist, in winter enhanced cyclonic and meso-cyclonic activity increases the potential of dynamical downscaling. In winter time the added value is more pronounced around Iceland and Greenland, south of Iceland and within the Gulf of Lyon/Mistral region. Summarizing the presented method can be easily applied for other ocean areas, making QuikSCAT a valuable tool to identify marine regions where dynamical downscaling adds value to surface marine wind speed. A detailed comparison of 10 m winds from the NCEP/NCAR and the newer NCEP/DOE-II reanalyses is presented in the annex, motivating the use

of the NCEP/NCAR reanalysis in the added value assessment.

# 1. Introduction

For the design and the maintenance of coastal protection measures, long and homogeneous time series of wind, waves and surge are necessary. They are needed to derive their statistics (in especially extreme value statistics) and to analyse long-term changes and trends. In addition these time series are used for a variety of applications, e.g. the design and maintenance of offshore installations such as platforms and wind farms.

However for marine areas, long and homogeneous data sets are rare. Regional atmospheric hindcasts obtained from regional climate models (RCMs) driven by global reanalyses form an alternative that can be used either to analyse long-term changes and trends (e.g., Fowler and Kilsby 2007; Weisse et al. 2005) or as forcing for other, e.g. hydrologic, wave or storm surge models (e.g. Gaslikova and Weisse 2006; Sotillo et al. 2005; Federico and Bellecci 2004; Kim and Lee 2003). This method of deriving smaller-scale information with a limited-area, high-resolution model using boundary conditions from a global model (such as a reanalysis) is called dynamical downscaling.

For regional hindcasts it is assumed, that they will provide an improved representation of processes on scales below the reanalysis' resolution such as e.g., fronts or mesoscale disturbances (e.g., Denis et al. 2002). Here, a crucial question is whether RCMs do indeed show an added value in comparison to the driving reanalysis. Concerning dynamically downscaled marine near-surface wind fields this question has been addressed in recent years in a number of studies. Using buoy wind speed measurements Sotillo et al. (2005), Kanamitsu

and Kanamaru (2007) and Winterfeldt and Weisse (2009) assessed the added value in the Mediterranean Sea, offshore California and in the eastern North Atlantic and the North Sea, respectively. For the Atlantic Basin northwest of Spain, especially far from coastal areas, Sotillo et al. (2005) found the NCEP/NCAR-reanalysis (hereafter: NRA\_R1) sufficient for realistically representing near-surface marine wind fields derived from in situ observations. On the other hand, Sotillo et al. (2005) found, that towards Mediterranean coastal regions with complex orography, NRA\_R1 near-surface wind fields are significantly enhanced by dynamical downscaling using RCMs, which is confirmed by Kanamitsu and Kanamaru (2007) for Californian coastal waters and by Winterfeldt and Weisse (2009) in the English Channel. However, for the North Sea coastal region, Winterfeldt and Weisse (2009) found no enhancement for “instantaneous“ wind speed but for the frequency distribution.

All the mentioned added value studies have in common that they are constrained to areas where buoy observations are available. This study focusses on the introduction of a method to assess the added value of RCM marine wind speed using satellite wind speed retrievals, namely QuikSCAT L2B12 winds, instead of buoy measurements. This method can be easily applied for all ocean regions. Using QuikSCAT wind speed retrievals as an estimate of real surface marine wind speed makes the added value assessment possible in remote areas far offshore where in-situ wind speeds are rarely measured. Even in regions where in-situ data is more frequent, gridded QuikSCAT data often enables a cheaper, easier and regularly spaced assessment than is possible with in-situ observations, irregularly distributed in space. For this study we generated a gridded version of QuikSCAT’s L2B12 swath data, which is then used in the added value assessment. Among others Kolstad (2008), Winterfeldt et al.

(2009), Accadia et al. (2007) and Ruti et al. (2008) showed that QuikSCAT gives good representation of 10 m wind speed in both the North Atlantic and the Mediterranean.

Besides the introduction of the QuikSCAT based added value assessment method, this study aims at the confirmation and generalization of the findings of Sotillo et al. (2005) and Winterfeldt and Weisse (2009). Additionally it enables the identification of areas in the eastern North Atlantic and European waters where dynamical downscaling with RCMs is skillful as far as surface marine wind speed is concerned. It is investigated whether dynamical downscaling is more skillful in different seasons and whether the added value is mainly determined by the finer resolution of the RCM land sea mask.

The paper is structured as follows. The analysed data sets and the method are described in Section 2. In Section 3 the added value of dynamical downscaling is assessed. Section 4 elaborates on the seasonality of the added value. Section 5 concludes the paper.

## 2. Data and Method

### *a. The NCEP/NCAR-reanalysis (NRA\_R1)*

The global reanalysis of atmospheric fields from National Centers of Environmental Prediction (NCEP) and National Center for Atmospheric Research (NCAR) involves the recovery of land surface, rawinsonde, pibal, aircraft, satellite, surface marine (ships, buoys, oil rigs, C-man platforms) and other data (Kalnay et al. 1996; Kistler et al. 2001). These

data are quality controlled and assimilated with a data assimilation scheme that is kept unchanged over the reanalysis period and does not use QuikSCAT data. Forecast 10 m horizontal wind speed components on a T62 gaussian grid with a grid spacing of  $1.875^\circ \times 1.875^\circ$  were obtained from the NOAA/OAR/ESRL PSD, Boulder, Colorado, USA, from their Web site at <http://www.cdc.noaa.gov/> for the comparison with QuikSCAT and modelled 10 m wind speed. The Forecast 10 m wind speed of the NCEP/NCAR reanalysis is used instead of the forecast 10 wind speed from the newer NCEP/DOE-II reanalysis (Kanamitsu et al. 2002) since the latter gives unrealistically high wind speeds. The differences between the 10 m wind speed from both reanalyses are presented in detail in Section 6 in the appendix.

*b. Regional atmospheric hindcast*

The SN-REMO hindcast with a horizontal grid spacing of  $0.5^\circ$  ( $\approx 50$  km) used in this study was generated and described by Feser et al. (2001). SN-REMO has an integration time step of five minutes, the output is given every hour. It is initialized and forced with the NRA\_R1, the modelled domain covers almost the whole eastern North Atlantic and is depicted in Figure 1. The SN-REMO hindcast uses a Type 2 dynamical downscaling according to the classification described by e.g. Castro et al. (2005) and Rockel et al. (2008).

REMO is a regional hydrostatic atmospheric model (Jacob and Podzun 1997). It has been developed from the Europa-Modell (EM) of the German Weather Service/Deutscher Wetterdienst (DWD), its dynamics are based on the primitive equations in a terrain-following hybrid coordinate system with 20 vertical layers. The prognostic variables of the model are

surface pressure, temperature, specific humidity, liquid water, and horizontal wind components. REMO is set up in its climatic mode using the same parameterization scheme as in the global climate model ECHAM4 (Roeckner et al. 1996). Vertical diffusion and turbulent surface fluxes are resolved as shown by the Monin-Obukhov theory (Louis 1979). Feser et al. (2001) generated the current 58-year (1958 - 2006) Central European hindcast by forcing REMO with the NRA\_R1 atmospheric global reanalysis with the spectral nudging method after von Storch et al. (2000) applied with the nudging parameter set to  $\alpha = 0.05$ . SN-REMO delivers diagnostic 10 m wind speed, meaning that the 10 m wind speed is calculated from the prognostic wind speed at the lowest model level, which is 32 m.

*c. QuikSCAT L2B12*

The US launched the SeaWinds scatterometer on the QuikSCAT mission satellite in 1999. The SeaWinds scatterometer is an active radar which transmits microwave pulses towards the earth's surface and receives the backscatter. Over the ocean the latter is largely determined by the roughness of the surface due to small centimeter-scale waves, which are assumed to be in equilibrium with the wind stress at the ocean surface (Tang et al. 2004). Multiple and simultaneous normalized radar cross section ( $\sigma_0$ ) values are obtained from the backscatter power at a single geographical location or wind vector cell (WVC) and converted to wind speed and direction measurements (10 m equivalent neutral winds) using a Geophysical Model Function (GMF, Callahan 2006).

For this study wind speed retrievals of the QuikSCAT Level 2B data at 12.5 km resolution (L2B12) are obtained from Jet Propulsion Laboratory (JPL), NASA website ([http://podaac-  
www.jpl.nasa.gov](http://podaac-<br/>www.jpl.nasa.gov)). Wind solutions that have not been modified by the Direction Interval Retrieval with Thresholded Nudging (DIRTH) algorithm after Stiles (1999) have been used and data flagged for rain after the Impact-based Multidimensional-Histogram (IMUDH, Huddleston and Stiles 2000) were discarded in this analysis.

Winterfeldt et al. (2009) compared L2B12 swath wind speed with buoy observations in the eastern North Atlantic and the North Sea and found it to give good representation of observed near-surface wind speed. They reported a root-mean-squared error (RMSE, L2B12 minus buoy) of  $1.7 \text{ m s}^{-1}$ , demonstrating that QuikSCAT's mission requirement of providing wind speed with an RMSE of  $2 \text{ m s}^{-1}$  is met for the eastern North Atlantic and the North Sea. QuikSCAT showed good agreement with buoy data for wind speeds up to  $20 \text{ m s}^{-1}$ .

#### 1) GRIDDED L2B12 DATA SET

While gridded L3B12 wind data are available from JPL, they are not considered in this analysis as the L2B12 data are clearly more accurate (Sharma and D'Sa 2008). Thus a gridded L2B12 data set was produced for the assessment which uses the same grid as the SN-REMO hindcast ( $0.5 \times 0.5^\circ$  grid spacing, domain depicted in Figure 1) and covers the years 2000 to 2007. Like the SN-REMO hindcast the gridded L2B12 uses a temporal resolution

of one hour. Whenever a QuikSCAT measurement is within 10 minutes of the full hour and  $0.1^\circ$  and  $0.06^\circ$  in longitudinal and latitudinal distance from a grid point it is assigned as a record to that grid point of the gridded L2B12 data set. These criteria result in at most two QuikSCAT records per day at any grid-point: one in the early morning and one in the evening.

*d. Method*

The gridded QuikSCAT data set and SN-REMO have the same grid dimensions. QuikSCAT is co-located with SN-REMO through the generation of the gridded data set with a co-location criteria of 10 minutes and  $0.1^\circ$  and  $0.06^\circ$  in longitudinal and latitudinal distance as described in the previous section. The NRA\_R1 is available every six hours and has a coarser grid spacing than SN-REMO. For the purpose of co-locating the NRA\_R1 with SN-REMO and QuikSCAT it is interpolated in time (to the one hour resolution of SN-REMO) and space onto the SN-REMO grid.

The gridded QuikSCAT L2B12 wind speed serves as estimate of real surface marine wind speed in the added value assessment. A modified Brier Skill Score (BSS) is used to test to what extent the regionally modelled wind gives a better reproduction of QuikSCAT wind speed than the NRA\_R1. The BSS is defined, e.g. von Storch and Zwiers (1999), by  $B = 1 - \sigma_F^2 \sigma_R^{-2}$ , where  $\sigma_F^2$  and  $\sigma_R^{-2}$  represent the error variances of the “forecast“  $F$  (the time series of regionally modelled wind speeds) and the reference “forecast“  $R$  (the time series of NRA\_R1 wind speeds). The error variances are computed relative to the same

predictand, here the respective time series of L2B12 wind speed. The modified version of the BSS used here simplifies the comparability of positive and negative scores and is given by

$$B = \begin{cases} 1 - \sigma_F^2 \sigma_R^{-2} & \sigma_F^2 \leq \sigma_R^2 \\ \sigma_R^2 \sigma_F^{-2} - 1 & \sigma_F^2 > \sigma_R^2. \end{cases} \quad (1)$$

By definition the Brier Skill Score can vary between  $-1$  (reference exactly matches the L2B12 observations) and  $+1$  (forecast exactly matches the L2B12 observations). Negative values indicate a better performance of the reference forecast (NRA\_R1), positive values indicate an added value of the regionally modelled winds in comparison to the NRA\_R1 time series. The added value assessment is carried out for the years 2000 to 2007.

Uncertainties in the assessment may be introduced by the different temporal and spatial resolutions of the QuikSCAT, NRA\_R1 and SN-REMO wind speeds. However this is partly inevitable as the aim of this analysis is to find out whether a medium resolution product (SN-REMO) is able to add value to the coarse resolution driver (NRA\_R1) by the means of comparing it with a high resolution data set (QuikSCAT). In the presented analysis the NRA\_R1 was time interpolated to one hour resolution. Subsampling the modelled and QuikSCAT wind speeds to the six-hour frequency prescribed by NRA\_R1 is an alternative approach. Winterfeldt and Weisse (2009) tested the sensitivity of the added value assessment to both methods, the resulting differences were negligible.

### 3. Results

The total amount of available co-locations between QuikSCATS's L2B12, the NRA\_R1 and SN-REMO for the period 2000 to 2007 is depicted in Figure 2(a). The mean QuikSCAT L2B12 wind speed from the total number of co-locations is displayed in Figure 2(b). Several features are discernible. In the Atlantic four wind speed nadirs are visible which have been reported by Kolstad (2008): between Iceland and Jan Mayen, between Jan Mayen and Spitsbergen, southeast of Spitsbergen between Hopen and Bear Island and to the southwest of Iceland. The latter wind speed nadir and the area of higher wind speed in the vicinity of the east Greenland topography have been attributed to wake effects downstream of the Greenland topography in westerly flow and to the barrier flow described by Moore and Renfrew (2005). The wind speed nadir in the northwestern most corner of the model domain is an artefact of the seasonal extension of the sea ice. In winter the wind speed retrieval is impossible due to sea ice, leading to a reduced amount of wind speed retrievals (bluish area in Figure 2(a)) and to a reduced mean wind speed since the wind speed in summer is generally lower.

Apart from the maximum wind speed in the storm track local wind speed maxima can be identified near the southern tip of Spitsbergen, northwest of the Galician coast, in the Mistral region in the Gulf of Lyon, in the Straits of Sicily and in the Aegean Sea. Local wind speed minima in the Mediterranean are located between the Iberian Peninsula and the Balears, in the Tyrrhenian Sea between Sardinia, Italy and Sicily, southeast of Sicily, in the Adriatic Sea and around Cyprus.

The number of co-locations in the wind speed range of 3 to 20 m s<sup>-1</sup>, which is reliably reproduced by L2B12 (e.g. Winterfeldt et al. 2009), is depicted in Figure 3(a). For almost the whole modelled North Atlantic more than 500 co-locations exist in this wind speed range. The number of co-locations is highest in the high latitudes and reduces southwards due to QuikSCAT's orbit specifications. Sea-ice contamination leads to a reduced number of co-locations east of Greenland. At any grid point in the model domain less than nine percent of all available L2B12 co-locations have wind speeds beyond 20 m s<sup>-1</sup> as illustrated by the isolines in Figure 3(a) which represents the wind speed percentile value corresponding to 20 m s<sup>-1</sup>. Less than 10 to 15 percent of all co-locations are below 3 m s<sup>-1</sup> (not shown).

The modified BSS after Equation 1 is displayed in Figure 3(b). In vast areas of the North Atlantic the BSS is negative indicating that dynamical downscaling does not add value there. The same holds for the interior of the Mediterranean, Baltic and Black Seas. Frequent occurrence of meso-scale phenomena like meso-cyclones (e.g. polar lows or meso-cyclones due to cyclogenesis in unstable cold air behind synoptic cyclones or a cold front), fronts, land sea breezes or orographic induced wind flow would increase the possibilities of RCMs to add value. Land sea breezes and orographic induced wind flow do not occur in the open ocean and are constrained to coastal areas. Accordingly there is hardly any possibility for SN-REMO to add value at the open ocean which is reflected by the negative Brier Skill Scores.

As indicated by positive BSS values SN-REMO is able to add value in coastal areas, mainly for those with complex coastlines/topography, especially in the Mediterranean, around the Iberian peninsula, between Iceland and Greenland, in the English Channel and the Irish Sea

and close to the coastlines of the Baltic and Black Seas. Here meso-scale phenomena are more common, especially in the Mediterranean Sea where local or regional winds triggered or modified by orography are frequent (e.g. Zecchetto and Biasio 2007), e.g. the Mistral area can be identified by positive BSS values.

These results confirm earlier results by Sotillo et al. (2005) and Winterfeldt and Weisse (2009). Their assessments with wind speed data from the buoys depicted in Figure 1 indicated an added value for coastal areas in the Mediterranean and the English Channel but hardly any for the North Sea coastal waters. They found no added value in the open ocean waters of the North Atlantic.

## 4. Seasonality of the added value

The seasonality of the added value of SN-REMO is investigated by subsampling the co-located data into winter (DJF), spring (MAM), summer (JJA) and fall (SON). The BSS for all seasons is depicted in Figure 4, the strongest interseasonal differences were determined between summer and winter. In general higher Brier Skill Scores stand out for the whole North Atlantic in winter time which coincides with stronger meso-scale activity during this season (e.g., Harold et al. (1999)) which can be attributed partly to Polar Lows and meso-cyclones developing behind synoptic cyclones in cold air outbreaks. Polar Lows (e.g. Zahn and von Storch 2008) occur mainly in winter time near the ice-edge, between and around Greenland and Iceland and between Spitsbergen and the Norwegian coast. For those areas the RCM adds value at more grid points in winter time. According to Harold et al. (1999)

the strongest seasonal changes in meso-cyclone activity occur near the Norwegian Coast, near the ice edge and south and southwest of Iceland. The large area of added value south of Iceland in winter time may be partly attributed to meso-cyclones generated behind the cold front of cyclones.

Strong interseasonal differences are detected for the Mediterranean and Black Seas. In winter the near-surface circulation in the north-west Mediterranean is characterized by a cyclonic meso-scale circulation (e.g. Millot 1987, 1991) in the Gulf of Lyon which is a seasonal characteristic induced by the frequent north-west winds or Mistral events. With the Mistral blowing more frequently from November to March (e.g. Zecchetto and Cappa 2001 and references therein) SN-REMO adds value in the whole Gulf of Lyon basin in winter time while adding value to a more constrained area in summer. In the land sea mask of the NRA\_R1 Corse, Sardinia, Sicily and South Italy are not existing, while they do in the land sea mask of SN-REMO, a fact that probably contributes strongest to the added value of SN-REMO in the lee of those land masses in dominating northwesterly winds. North of Tunisia and in the Straits of Sicily increased wind speed associated with barrier flow close to the Atlas Mountains and gap flow in the Straits is discernible in Figure 2(b). In the wake of the Atlas Mountains east of Tunisia, meso-scale anticyclonic structures are reported by Accadia et al. (2007) which may be the reason for the added value to be visible there in all seasons. After Zecchetto and Biasio (2007) this anticyclonic area is particularly wide and deep in the spring and summer, when the Saharan low pressure system and the wind shielding effect of the Atlas Mountains under northerly winds concur to enhance its strength.

The etesian is a regional scale northerly wind in the Aegean Sea. In summer time when the etesians are strongest, steadiest and their wind speed variability is lowest (Zecchetto and Biasio 2007) SN-REMO can not add value in the etesian region north and south-east of Crete and Rhodes. In the Black Sea an area of positive BSS stands out stretching from the northern shores of Turkey to the island of Crimea in winter time. This feature is entirely missing in summer. Whether it is due to the western Black Sea anticyclone (Efimov and Shokurov 2002) and/or the stronger synoptic scale activity in winter interacting with the surrounding orography leading to stronger but directionally unsteady winds as reported by Zecchetto and Biasio (2007) remains unclear. In addition, Accadia et al. (2007) reported strong directional differences between the winds from the RCM QBolam and QuikSCAT in the western Black Sea in winter time.

We have seen that SN-REMO is unable to add value in the open ocean. It is important to note that the open ocean areas of the North Atlantic coincide with the interior of the model domain. Therefore the loss in value is a combination of the low frequency of meso-scale features in the open ocean and the position within the interior of the model domain far from the lateral boundary forcing of the reanalysis, which may lead to a significant deviation of large-scale features such as cyclone tracks or the location of pressure systems from those in the reanalysis (e.g., von Storch et al. 2000). The spectral nudging technique after von Storch et al. (2000) used for the SN-REMO simulation attempts to overcome these shortcomings and partly succeeds in it since the loss in value is lower for spectrally nudged simulations than for their unnudged counterparts (Winterfeldt and Weisse 2009). Nevertheless the spectral nudging technique needs to be optimised because large-scale value is still lost in the model

interior. The results in winter time are promising in a sense that dynamical downscaling with RCMs may add value even in the open ocean. However an improved coupling of the RCM to the large-scale forcing retaining the large-scale value of the reanalysis needs to be achieved first.

## 5. Discussion and Conclusion

A remote sensing based method to investigate the added value of marine RCM wind speed is presented: The capability of the dynamical downscaling approach to add value for surface marine wind speed in comparison to the reanalysis wind speed forcing is assessed by the comparison with QuikSCAT Level 2B 12.5 km (L2B12) swath data in European waters for 2000 to 2007. The dynamical downscaling approach is represented by a regional simulation with the RCM REMO which downscales the global NCEP/NCAR reanalysis using the spectral nudging technique after von Storch et al. (2000). In the wind speed range QuikSCAT L2B12 is reliably reproducing (3-20 m s<sup>-1</sup>), dynamically downscaled wind speed does not show an added value in “open ocean“ areas. However in coastal areas with complex topography the regional models show an added value, especially around Iceland and the Iberian peninsula and in the Mediterranean, Baltic and Irish Seas.

This analysis confirms the findings of previous in-situ data based studies on the added value by Sotillo et al. (2005) and Winterfeldt and Weisse (2009). In agreement with Sotillo

et al. (2005) this study shows that dynamical downscaling is capable to add value in coastal areas in the Mediterranean especially in the lee of islands, e.g. Corse, Sardinia, Sicily and the Aegean islands which are better resolved by REMO's land sea mask, and in areas of regional wind regimes as for the Gulf of Lyon (Mistral) and for the anticyclone in the wake of the Atlas Mountains east of Tunisia. However, in the etesian region north and south-east of Crete and Rhodes SN-REMO is unable to add value in summer when the etesians are strongest and steadiest. Winterfeldt and Weisse (2009) reported no significant added value for instantaneous wind speed in the North Sea coastal region while they found added value in the English Channel. Both findings are confirmed by this study. Stronger cyclonic and meso-cyclonic activity in winter increases the potential of dynamical downscaling. Areas of enhanced added value can be attributed partly to Polar Lows and meso-cyclones developing behind synoptic cyclones in cold air outbreaks.

Several error sources relevant to this study exist: Apart from the QuikSCAT error of 2 m/s (e.g., Winterfeldt et al. (2009)), the direct comparison of SN-REMO and NRA\_R1 wind speed with microwave winds is erroneous, as QuickSCAT wind speed retrievals represent equivalent neutral 10 m wind, while SN-REMO and NRA\_R1 give diagnostic 10 m wind speed at modelled stability conditions. At sites where strong unstable or stable stratification occurs frequently equivalent neutral 10 m wind deviates from actual stability dependent wind, which, aside from the dynamics, could have a influence on the seasonal variations of the BSS presented in Section 4. While a detailed quantification of this stability effect is beyond the scope of this paper, a high level assessment was made converting winds from two buoys, namely K1 and Ems (Fig. 1) both to the 10m equivalent neutral wind (EQNW) after

Liu and Tang (1996) and the stability dependent wind (STDW) according to the bulk-flux algorithm after Fairall et al. (2003). The seasonal BSS values were then determined for both conversion methods. At K1 no dependence of the BSS on the conversion method (EQNW or STDW) is found as illustrated in Table 1, which is plausible, since for the open ocean the logarithmic wind profile is well known from observations (e.g., Edson and Fairall 1998). At K1 the stability conditions are near neutral during the whole year as indicated by the air/sea temperature difference at K1 depicted for winter (DJF) in Figure 5(a) and summer (JJA) in Figure 5(b). Thus, the seasonal BSS values determined with QuikSCAT's equivalent neutral winds can be considered realistic for offshore locations.

The air/sea temperature difference and hence the stratification often shows higher seasonal variations at nearshore locations. While the stratification at the nearshore lightship Ems is near neutral during summer as depicted in Figure 5(d), large stability variations exist in autumn and winter (Figure 5(c)). Therefore EQNW based BSS values deviate more strongly from STDW ones at Ems in autumn and winter as illustrated in Table 1. However, the qualitative result is not influenced at Ems (lower BSS values in spring and summer, higher ones in autumn and winter). Nevertheless, a qualitative dependence of the seasonal BSS fluctuations on seasonal stability variations cannot be generally excluded for coastal areas.

#### *Acknowledgments.*

The authors thank the three anonymous reviewers for their helpful suggestions. The authors would like to thank B. Gardeike and J. Bhend for rearranging the figures and the

following institutions and people who supplied and helped with the data: QuikSCAT Level 2B data was provided by JPL, NASA (<http://podaac-www.jpl.nasa.gov>), SN-REMO data by F. Feser (GKSS), NRA\_R1 data provided by the NOAA/OAR/ESRL PSD, Boulder, Colorado, USA (<http://www.cdc.noaa.gov/>). For supplying observation data we like to thank Met Office UK, especially B. Hall for his help, DNMI, KNMI, DWD and BSH. We appreciated the fruitful discussions with Hans von Storch and the helpful comments on regional modelling by F. Feser and B. Rockel.

## REFERENCES

- Accadia, C., S. Zecchetto, A. Lavagnini, and A. Speranza, 2007: Comparison of 10-m wind forecasts from a regional area model and QuikSCAT Scatterometer wind observations over the Mediterranean Sea. *Monthly Weather Rev.*, **135** (5), 1945–1960.
- Callahan, P. S., 2006: QuikSCAT Science Data Product User’s Manual V3.0. JPL Document D-18053-RevA, Jet Propulsion Laboratory, California Institute of Technology. URL [ftp://podaac.jpl.nasa.gov/pub/ocean\\_wind/quikscat/doc/QSUG\\_v3.pdf](ftp://podaac.jpl.nasa.gov/pub/ocean_wind/quikscat/doc/QSUG_v3.pdf).
- Castro, C. L., R. A. Pielke, and G. Leoncini, 2005: Dynamical downscaling: Assessment of value retained and added using the Regional Atmospheric Modeling System (RAMS). *J. Geophysical Research-atmospheres*, **110** (D05108), doi:10.1029/2004JD004721.
- Denis, B., R. Laprise, D. Caya, and J. Cote, 2002: Downscaling ability of one-way nested regional climate models: the Big-Brother experiment. *Climate Dynamics*, **18** (8), 627–646.
- Edson, J. B. and C. W. Fairall, 1998: Similarity relationships in the marine atmospheric surface layer for terms in the TKE and scalar variance budgets. *J. Atmos. Sci* **55**, 2311–2328.
- Efimov, V. V. and M. V. Shokurov, 2002: Spatiotemporal structure of the surface wind field over the Black sea. *Izvestiya Atmospheric Oceanic Phys.*, **38** (4), 421–430.
- Fairall, C. W., E. F. Bradley, J. E. Hare, A. A. Grachev, and J. B. Edson, 2003: Bulk

- parameterization of air-sea fluxes: Updates and verification for the COARE algorithm. *Journal of Climate*, **16**, 571–591.
- Federico, S. and C. Bellecci, 2004: Sea storms hindcast around Calabrian coasts: Seven cases study. *Nuovo Cimento Della Societa Italiana Di Fisica C-geophysics Space Phys.*, **27 (2)**, 179–203.
- Feser, F., R. Weisse, and H. von Storch, 2001: Multi-decadal atmospheric modeling for Europe yields multi-purpose data. *Eos Trans. Amer. Geophys. Union*, **82**, 305 – 310.
- Fowler, H. J. and C. G. Kilsby, 2007: Using regional climate model data to simulate historical and future river flows in northwest England. *Climatic Change*, **80 (3-4)**, 337–367.
- Gaslikova, L. and R. Weisse, 2006: Estimating near-shore wave statistics from regional hindcasts using downscaling techniques. *Ocean Dynamics*, **56**, 26–35.
- Harold, J. M., G. R. Bigg, and J. Turner, 1999: Mesocyclone activity over the Northeast Atlantic. Part 2: An investigation of causal mechanisms. *Int. J. Climatology*, **19 (12)**, 1283–1299.
- Hong, S.-Y. and H.-L. Pan, 1996: Nonlocal boundary layer vertical diffusion in a medium-range forecast model. *Mon. Wea. Rev.*, **124**, 2322–2339.
- Huddleston, J. N. and B. W. Stiles, 2000: Multidimensional histogram (MUDH) rain flag. Product Description Version 3.0, Jet Propulsion Laboratory, California Institute of Technology, Pasadena, CA. URL [ftp://podaac.jpl.nasa.gov/pub/ocean\\_wind/quikscat/L2B/doc/MUDH\\_Description\\_V3.pdf](ftp://podaac.jpl.nasa.gov/pub/ocean_wind/quikscat/L2B/doc/MUDH_Description_V3.pdf).

- Jacob, D. and R. Podzun, 1997: Sensitivity studies with the regional climate model REMO. *Meteor. Atmos. Phys.*, **63**, 119–129.
- Kalnay, E., et al., 1996: The NCEP/NCAR 40-year Reanalysis Project. *Bull. Amer. Meteorol. Soc.*, **77 (3)**, 437–471.
- Kanamitsu, M., 1989: Description of the NMC Global Data Assimilation and Forecast System. *Weather Forecasting*, **4**, 334–342.
- Kanamitsu, M., W. Ebisuzaki, J. Woollen, S. K. Yang, J. J. Hnilo, M. Fiorino, and G. L. Potter, 2002: NCEP-DOE AMIP-II Reanalysis (R-2). *Bulletin Am. Meteorol. Soc.*, **83 (11)**, 1631–1643.
- Kanamitsu, M. and H. Kanamaru, 2007: Fifty-seven-year California Reanalysis Downscaling at 10 km (CaRD10). Part I: System detail and validation with observations. *J. Climate*, **20**, 5553–5571.
- Kanamitsu, M., et al., 1991: Recent changes implemented into the global forecast system at NMC. *Weather Forecasting*, **6 (3)**, 425–435.
- Kara, A. B., A. J. Wallcraft, C. N. Barron, H. E. Hurlburt, and M. A. Bourassa, 2008: Accuracy of 10 m winds from satellites and NWP products near land-sea boundaries. *J. Geophysical Research-oceans*, **113 (C10)**, C10 020.
- Kim, J. and J. E. Lee, 2003: A multiyear regional climate hindcast for the Western United States using the mesoscale atmospheric simulation model. *J. Hydrometeorology*, **4 (5)**, 878–890.

- Kistler, R., et al., 2001: The NCEP-NCAR 50-year reanalysis: Monthly means CD-ROM and documentation. *Bulletin Am. Meteorol. Soc.*, **82**, 247–267.
- Kolstad, E. W., 2008: A QuikSCAT climatology of ocean surface winds in the Nordic seas: Identification of features and comparison with the NCEP/NCAR reanalysis. *J. Geophysical Research-atmospheres*, **113 (D11106)**, doi:10.1029/2007JD008918.
- Liu, W. T. and W. Tang, 1996: Equivalent neutral wind. JPL Publication 96-17, Jet Propulsion Laboratory, California Institute of Technology, Pasadena, CA. URL <http://airsea-www.jpl.nasa.gov/publication/paper/Liu-Tang-1996-jpl.pdf>.
- Louis, J., 1979: A parametric model of vertical eddy fluxes in the atmosphere. *Bound.-Layer Meteor.*, **17**, 187–202.
- Millot, C., 1987: Circulation in the western mediterranean-sea. *Oceanologica Acta*, **10 (2)**, 143–149.
- Millot, C., 1991: Mesoscale and seasonal variabilities of the circulation in the western mediterranean. *Dynamics Atmospheres Oceans*, **15 (3-5)**, 179–214.
- Moore, G. W. K. and I. A. Renfrew, 2005: Tip jets and barrier winds: A QuikSCAT climatology of high wind speed events around greenland. *J. Climate*, **18 (18)**, 3713–3725.
- NASA, 1976: *U.S. Standard Atmosphere*. NOAA, NASA and USAF, U.S. Government Printing Office, Washington, D.C.
- NOAA/NMC, 1988: *NOAA/NMC Development Division: Documentation of the NMC global*

*model*. [Available from NOAA/NCEP Environmental Modeling Center, 5200 Auth Rd., Washington, DC 20233].

Rockel, B., C. L. Castro, R. A. Pielke, H. von Storch, and G. Leoncini, 2008: Dynamical Downscaling: Assessment of Model System Dependent Retained and Added Variability for two Different Regional Climate Models. *J. Geophysical Research*, **113** (D21107), doi: 10.1029/2007JD009461.

Roeckner, E., et al., 1996: The atmospheric general circulation model ECHAM4: Model description and simulation of present-day climate. Technical Report 218, Max-Planck Inst. für Meteorol., Hamburg, Germany, 90 pp.

Ruti, P. M., S. Marullo, F. D’Ortenzio, and M. Tremant, 2008: Comparison of analyzed and measured wind speeds in the perspective of oceanic simulations over the Mediterranean basin: Analyses, QuikSCAT and buoy data. *J. Marine Systems*, **70**, 33–48.

Sharma, N. and E. D’Sa, 2008: Assessment and analysis of QuikSCAT vector wind products for the Gulf of Mexico: A long-term and hurricane analysis. *Sensors*, **8** (3), 1927–1949.

Sotillo, M., A. Ratsimandresy, J. Carretero, A. Bentamy, F. Valero, and F. Gonzalez-Rouco, 2005: A high-resolution 44-year atmospheric hindcast for the Mediterranean Basin: Contribution to the regional improvement of global reanalysis. *Climate Dyn.*, **25**, 219–236.

Stiles, B. W., 1999: Special Wind Vector Data Product: Direction Interval Retrieval with Threshold Nudging (DIRTH). Product Description Version 1.1, Jet Propulsion Laboratory, California Institute of Technology. URL [ftp://podaac.jpl.nasa.gov/ocean\\_wind/quikscat/L2B12/doc/Dirth-Product-Description.pdf](ftp://podaac.jpl.nasa.gov/ocean_wind/quikscat/L2B12/doc/Dirth-Product-Description.pdf).

- Tang, W. Q., W. T. Liu, and B. W. Stiles, 2004: Evaluations of high-resolution ocean surface vector winds measured by QuikSCAT scatterometer in coastal regions. *Ieee Transactions On Geoscience Remote Sensing*, **42 (8)**, 1762–1769.
- von Storch, H., H. Langenberg, and F. Feser, 2000: A spectral nudging technique for dynamical downscaling purposes. *Mon. Wea. Rev.*, **128**, 3664–3673.
- von Storch, H. and F. Zwiers, 1999: *Statistical Analysis in Climate Research*. Cambridge University Press.
- Weisse, R., H. Storch, and F. Feser, 2005: Northeast Atlantic and North Sea storminess as simulated by a Regional Climate Model 1958-2001 and comparison with observations. *J. Climate*, **18**, 465–479.
- Winterfeldt, J., A. Andersson, C. Klepp, S. Bakan, and R. Weisse, 2009: Comparison of HOAPS, QuikSCAT and Buoy Wind Speed in the Eastern North Atlantic and the North Sea. *IEEE Transactions On Geoscience Remote Sensing*, **48 (1)**, 338–348, doi:10.1109/TGRS.2009.2023982.
- Winterfeldt, J. and R. Weisse, 2009: Assessment of value added for surface marine wind speed obtained from two Regional Climate Models (RCMs). *Monthly Weather Review*, **137 (9)**, 2955–2965, doi:10.1175/2009MWR2704.1.
- Zahn, M. and H. von Storch, 2008: A long-term climatology of North Atlantic polar lows. *Geophys. Res. Lett.*, **35 (L22702)**, doi:10.1029/2008GL035769.
- Zecchetto, S. and F. D. Biasio, 2007: Sea surface winds over the Mediterranean basin from

satellite data (2000-04): Meso- and local-scale features on annual and seasonal time scales.

*J. Appl. Meteorology Climatology*, **46** (6), 814–827.

Zecchetto, S. and C. Cappa, 2001: The spatial structure of the Mediterranean Sea winds revealed by ERS-1 scatterometer. *Int. J. Remote Sensing*, **22** (1), 45–70.

## APPENDIX

### **6. Comparison of 10 m wind speed from NRA\_R1 and NRA\_R2**

Both the NCEP/NCAR Reanalysis (NRA\_R1, Kalnay et al. 1996; Kistler et al. 2001) and the the newer reanalysis from NCEP and the Department of Energy (DOE), the NCEP-DOE Reanalysis II (hereafter: NRA\_R2, Kanamitsu et al. 2002) deliver forecast 10 m horizontal wind speed. Often the different 10m forecasts are treated as interchangeable products, however there is a strong systematic bias between the forecast 10 m wind speed of both reanalyses, as this section shows. A comparison with marine in situ observations is presented which indicates a major inconsistency in the NRA\_R2 reanalysis/forecast system and that the 10 m wind speed forecast of the NRA\_R1 is closer to reality.

*a. Introduction*

Briefly the NRA\_R1 reanalysis assimilation scheme works as follows: The 6h forecast started from the previous analysis serves as the first-guess field. In the spectral statistical interpolation (SSI) step, differences between the assimilated observations and the first guess-field are determined, which deliver the analysis correction. The analysis is updated with the analysis correction in the next step. The initial field for the next 6h forecast is determined from the analysis in the fourth step. Finally the forecast creates the guess for the next analysis step. The forecast model used is the T62/28-level NCEP global spectral model. The details of the model dynamics and physics are described in NOAA/NMC, Kanamitsu (1989) and Kanamitsu et al. (1991)

The NRA\_R2 provided upgrades to the forecast model Kanamitsu et al. (2002). The implementation of the Hong-Pan planetary boundary layer non-local vertical diffusion scheme Hong and Pan (1996), a smoothed orography and different convective parameterizations may cause changes in the wind speed relative to NRA\_R1. Both reanalyses are intercompared concerning the forecast wind speed at 10 m height. Main focus is the comparison with in-situ wind speed observations at 10 m height in the eastern North Atlantic and the North Sea in the year 1998.

*b. Method*

The buoy data set used for this analysis is identical to that used by Winterfeldt and Weisse (2009) and is depicted in Figure 1. The in-situ wind speed observations were converted to

10 m height using the COARE bulk flux algorithm in version 3.0b after Fairall et al. (2003). For the comparison the 10 m wind speed forecasts of both the NRA\_R1 and NRA\_R2 are bilinearly interpolated onto the locations of the in-situ measurements. In addition, both the NRA\_R1 and NRA\_R2 forecasts were time interpolated linearly to the one hour resolution given by the observations.

*c. Results and Discussion*

The results of the comparison are displayed in Figure 6. In general a large positive bias between the NRA\_R2 and the NRA\_R1 in the order of  $2 \text{ m s}^{-1}$  can be inferred (see also Figure 7(a)). Far offshore at K1, RARH, K5, FRIGG and F3 the NRA\_R1 agrees better with observed mean wind speed while the NRA\_R2 overestimates 10 m wind speed by up to  $2 \text{ m s}^{-1}$  ( $3 \text{ m s}^{-1}$  at K5 due to both NRA\_R2 large bias and too low wind speed measurements at K5). Closer to the coast and, especially within the English Channel, the NRA\_R2 shows a much better agreement with the observations.

The latter represents a highly unplausible result, because both forecasts calculate wind speed over approximately  $200 \times 200 \text{ km}$  wide grid boxes and can therefore hardly resolve the topography within the English Channel. At each grid box within the English Channel some kind of smoothed topography, averaged over the water and adjacent land surfaces, is used in both forecasts. As a result the surface roughness will be higher and consequently the forecast wind speed within the English Channel should be lower than that measured by the English Channel lightships Chan, GRW and Sand. While this is the case for the NRA\_R1,

the NRA\_R2 gives mean wind speeds comparable to the in-situ data.

Similarly, where topographic features, averaged over a forecast grid cell, are relatively homogeneous (such as for open waters) near-surface wind speed is expected to show less variance and in-turn a better agreement between in-situ and forecast wind speed might be expected. While again this is the case for the NRA\_R1, it is not for the NRA\_R2. While representing an average over 200x200 km with an integration time step of 20 min, the NRA\_R2 forecast gives wind speed variabilities higher than observed for 9 of 12 cases, which is highly unpalatable. The RMSE of the NRA\_R2 10 m forecast again shows its counterintuitive behaviour, since it gives lower RMSE values near coastlines it cannot resolve and higher RMSE for areas far offshore. As depicted in Figure 7(b), the strong bias between the NRA\_R2 and NRA\_R1 10 m wind speed forecasts is not constrained to the Northeast Atlantic. With the exception of the subtropical latitudes around 30° and some patches in the Antarctic, the NRA\_R2 shows too high 10 m wind speed as compared to the NRA\_R1. This positive bias peaks to 1.5 m s<sup>-1</sup> and above in and around the Antarctic and on the Eurasian and North American land masses. The overestimation of near-surface marine wind speed of the NRA\_R2 is the reason why Kara et al. (2008) could not improve near coastal winds of the NRA\_R2 with their creeping sea-fill technique while they could improve the near coastal winds of the ERA-40 reanalysis and the NOGAPS forecast model. In case of the NRA\_R2 the creeping sea-fill method interpolates “stronger winds from the interior ocean to the coastal regions. In other words, land contamination improves the accuracy of the NRA\_R2 product over the sea near the coast by weakening the generally excessive winds in the ocean interior “ (Kara et al. 2008).

In 1998, the mean sea level pressure in the investigated area is similar to the 1013 hPa given for the U.S. Standard Atmosphere after NASA(not shown). Thus, in agreement with the standard atmosphere, the 1000 hPa level is expected to be in average at a height of around 100 m. Consequently, according to the vertical wind speed profile in the surface layer, the wind speed at 1000 hPa is in average higher than that at 10 m height. For 1998, the differences of the annual averages of the reanalysed 1000 hPa and forecast 10 m wind speed are depicted in Figure 8. While the NRA\_R1 shows higher wind speeds on the 1000 hPa level (Figure 8(a)), the NRA\_R2 forecast wind speed in 10 m height even exceeds the reanalysed wind speed at the 1000 hPa level (Figure 8(b)), indicating a major inconsistency in the NRA\_R2 reanalysis/forecast system, as far as near-surface wind speed is concerned.

Both reanalyses show similar wind speed patterns at 1000 hPa, which is not surprising given that both reanalyses assimilate similar marine near-surface wind speed observations. In detail, the differences are much smaller than the differences between the 10 m wind speed forecasts and have the opposite sign (Figure 8(c)). These findings indicate on the one hand, that the NRA\_R2 10 m wind speed forecast is not representative for the near-surface wind field of the NRA\_R2 reanalysis. On the other hand, a problem within the Hong-Pan planetary boundary layer non-local vertical diffusion scheme Hong and Pan (1996) implemented in the NRA\_R2 forecast model is indicated. Additionally, the strong bias may be attributed at least in part to the different convective parameterizations leading to more intense storms in the NRA\_R2 (W. Ebisuzaki, Climate Prediction Center, NCEP, pers. comment).

The effects are also visible in the wind speed frequency distributions in Figure 9. While

the bias between both forecasts is similar at all stations, the bias between the NRA\_R2 forecasts and in-situ wind speed is strongest for open ocean areas as depicted in Figure 9(a). The latter bias is lowered in coastal areas by the increasing influence of the surrounding land mass on the forecast wind speed, leading to apparently well matched wind speed frequency distributions in the German Bight and especially in the English Channel as illustrated in Figures 9(b) and 9(c).

# List of Figures

1	Model domain and land sea mask of SN-REMO. The buoy data sets used in the added value assessments by Sotillo et al. (2005) and Winterfeldt and Weisse (2009) are depicted. . . . .	34
2	Total number of co-locations between QuikSCAT L2B12, NRA_R1 and SN-REMO (left) and mean wind speed of co-located QuikSCAT L2B12 retrievals (right). . . . .	35
3	a) Number of co-locations between QuikSCAT L2B12, NRA_R1 and SN-REMO for the wind speed range 3 to 20 m s <sup>-1</sup> and the years 2000 to 2007. The isolines show the percentile values corresponding to a wind speed of 20 m s <sup>-1</sup> . b) Modified Brier Skill Score after Equation 1 using QuikSCAT L2B12 as “truth“, NRA_R1 as reference “forecast“ and SN-REMO as “forecast“. . .	36
4	Seasonal BSS after Equation 1 using QuikSCAT L2B12 as “truth“, NRA_R1 as reference “forecast“ and SN-REMO as “forecast“ for a) winter, b) spring, c) summer and d) autumn. . . . .	37
5	Histogram of temperature difference between air and sea temperature (Ta-Ts) at K1 (top) and Ems (bottom) in winter (DJF, left) and summer (JJA, right) in 2002. The temperature difference is an indicator for atmospheric stability, negative/positive values indicate a unstable/stable stratification. . . . .	38
6	Comparison of in-situ wind speed with 10 m wind speed forecasts of NRA_R1 and NRA_R2 in 1998: a) mean wind speed, b) its standard deviation and c) root-mean-square error. . . . .	39

7	Bias between the 10 m forecast wind speed of the NRA_R2 and NRA_R1 in the eastern North Atlantic and the North Sea (left) and globally (right) in 1998 . . . . .	40
8	Comparison of the reanalysed 1000 hPa and forecast (fc) 10 m wind speed of both reanalyses in 1998: a) NRA_R1: 1000 hPa - 10 m fc, b) NRA_R2: 1000 hPa - 10 m fc, c) 1000 hPa: NRA_R2 - NRA_R1. . . . .	41
9	Comparison of percentile-percentile distributions of 10 m wind speed from NRA_R1 and NRA_R2 forecasts (y-axis) and in-situ data (x-axis) at a) the buoy RARH as an open ocean station and b) the light ships DeBu and c) Channel as coastal stations. . . . .	42

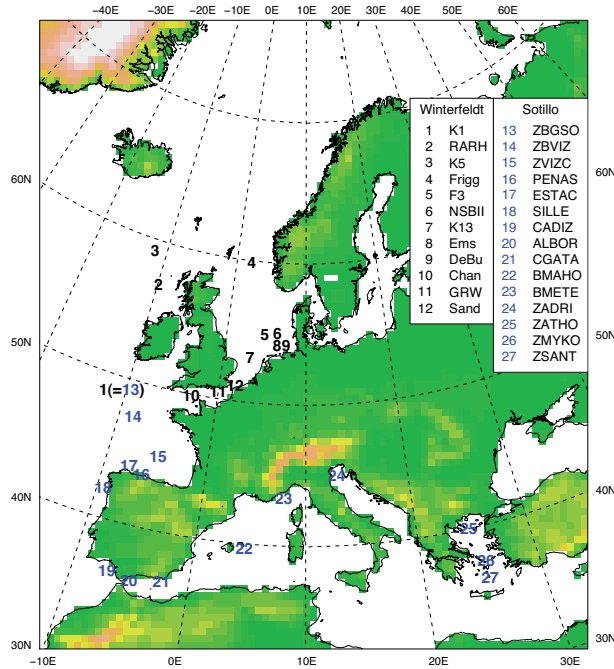


FIG. 1. Model domain and land sea mask of SN-REMO. The buoy data sets used in the added value assessments by Sotillo et al. (2005) and Winterfeldt and Weisse (2009) are depicted.

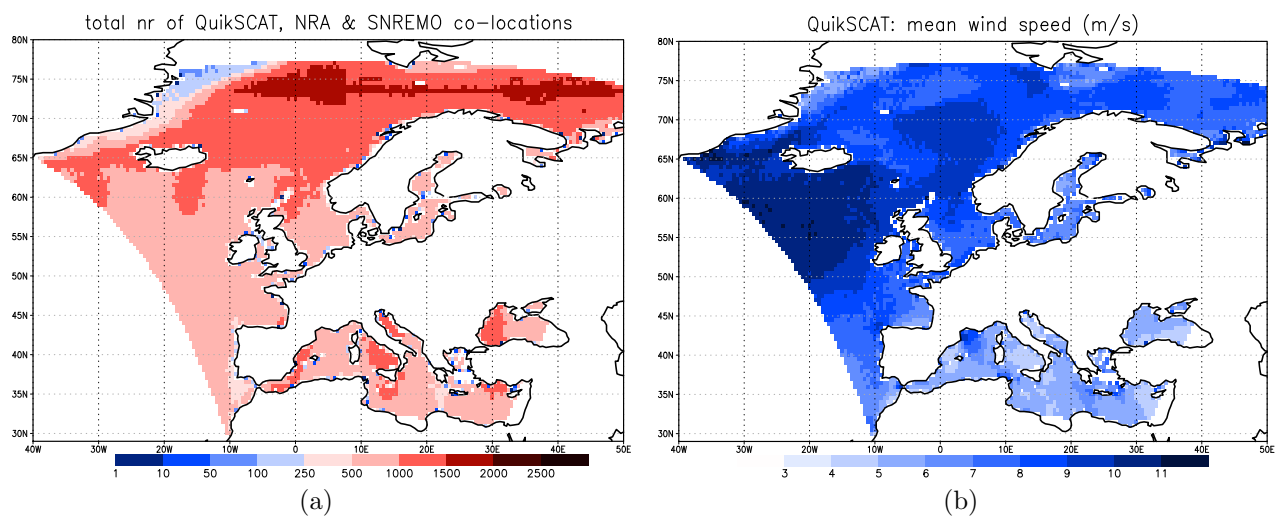


FIG. 2. Total number of co-locations between QuikSCAT L2B12, NRA\_R1 and SN-REMO (left) and mean wind speed of co-located QuikSCAT L2B12 retrievals (right).

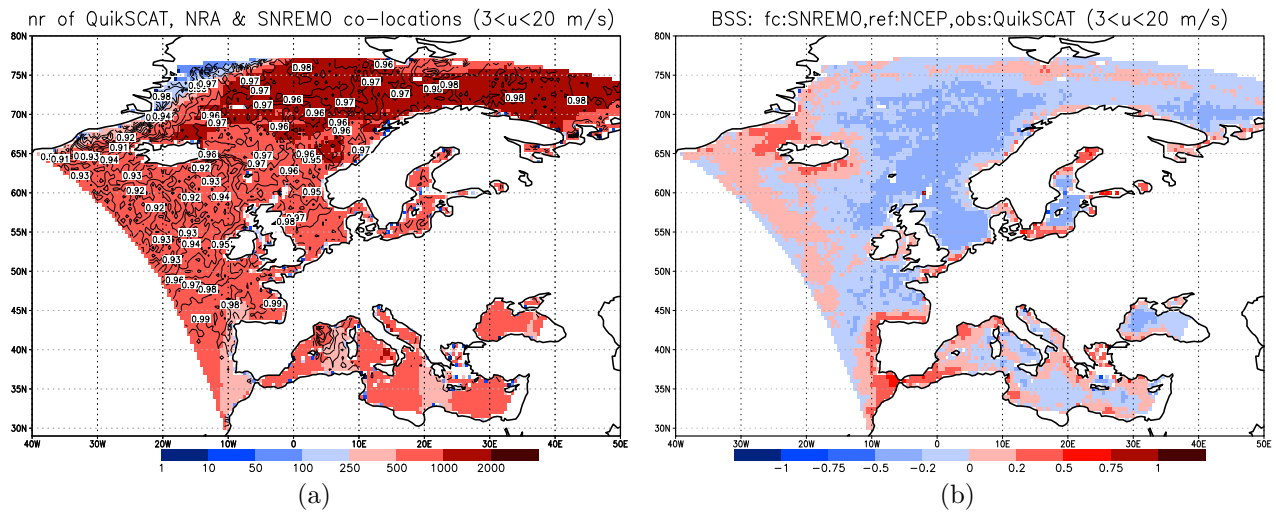


FIG. 3. a) Number of co-locations between QuikSCAT L2B12, NRA\_R1 and SN-REMO for the wind speed range 3 to 20  $\text{m s}^{-1}$  and the years 2000 to 2007. The isolines show the percentile values corresponding to a wind speed of 20  $\text{m s}^{-1}$ . b) Modified Brier Skill Score after Equation 1 using QuikSCAT L2B12 as “truth“, NRA\_R1 as reference “forecast“ and SN-REMO as “forecast“.

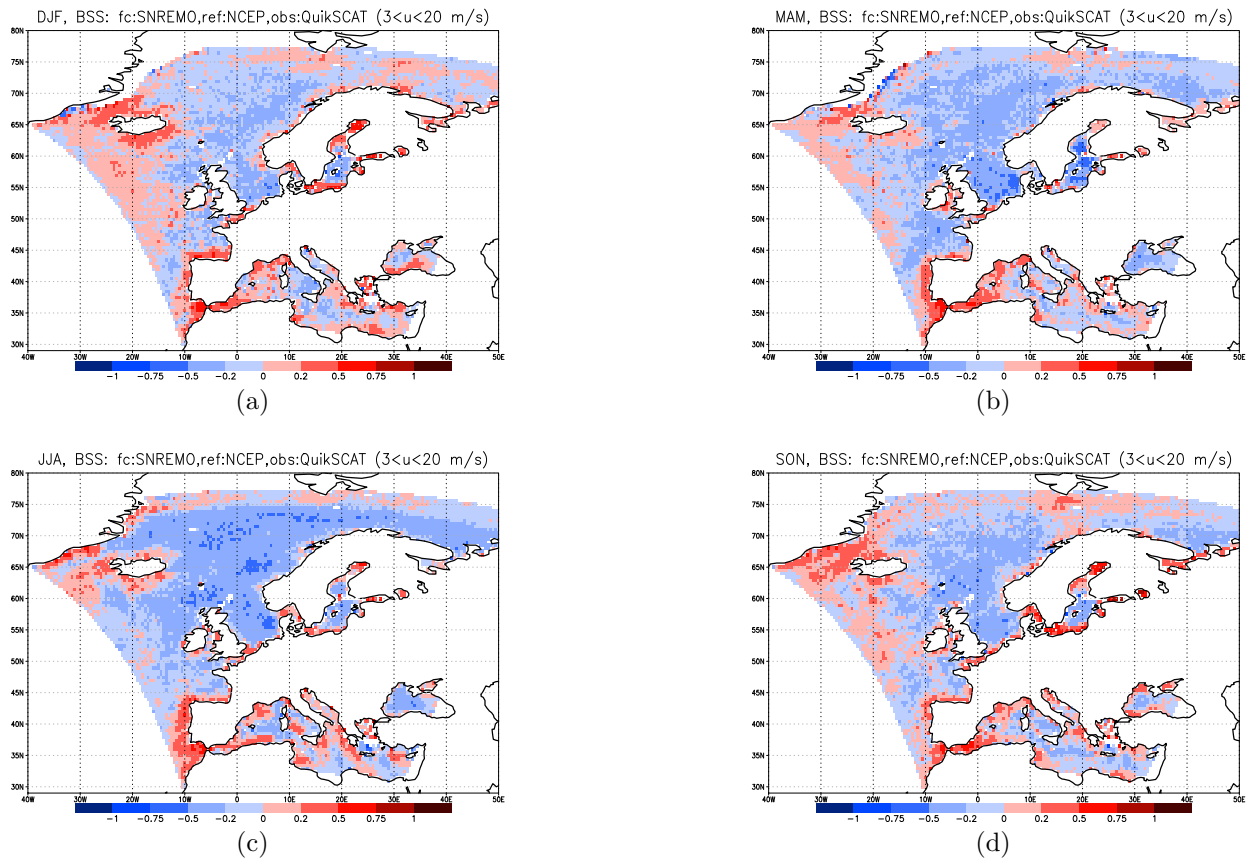
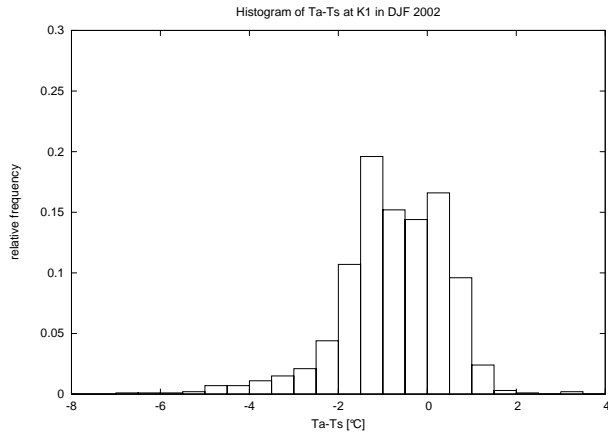
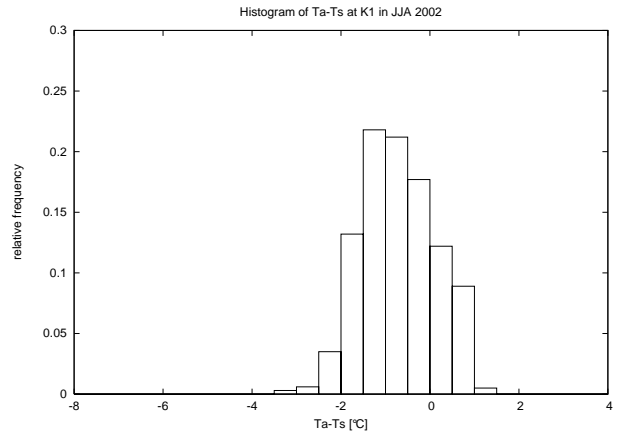


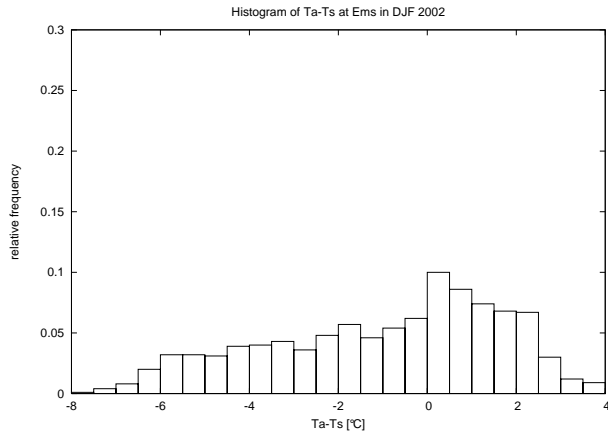
FIG. 4. Seasonal BSS after Equation 1 using QuikSCAT L2B12 as “truth“, NRA\_R1 as reference “forecast“ and SN-REMO as “forecast“ for a) winter, b) spring, c) summer and d) autumn.



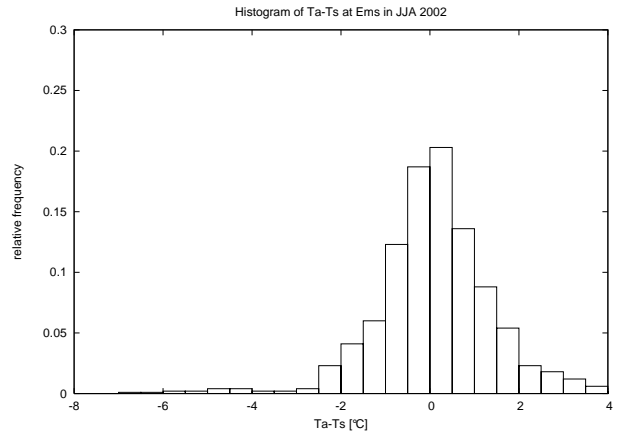
(a)



(b)

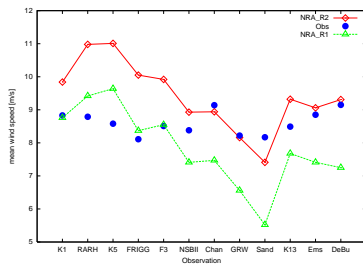


(c)

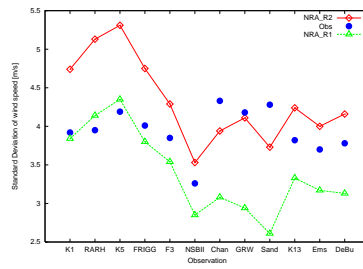


(d)

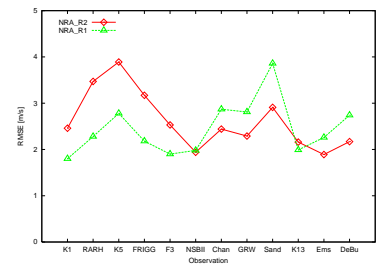
FIG. 5. Histogram of temperature difference between air and sea temperature ( $T_a - T_s$ ) at K1 (top) and Ems (bottom) in winter (DJF, left) and summer (JJA, right) in 2002. The temperature difference is an indicator for atmospheric stability, negative/positive values indicate a unstable/stable stratification.



(a)



(b)



(c)

FIG. 6. Comparison of in-situ wind speed with 10 m wind speed forecasts of NRA\_R1 and NRA\_R2 in 1998: a) mean wind speed, b) its standard deviation and c) root-mean-square error.

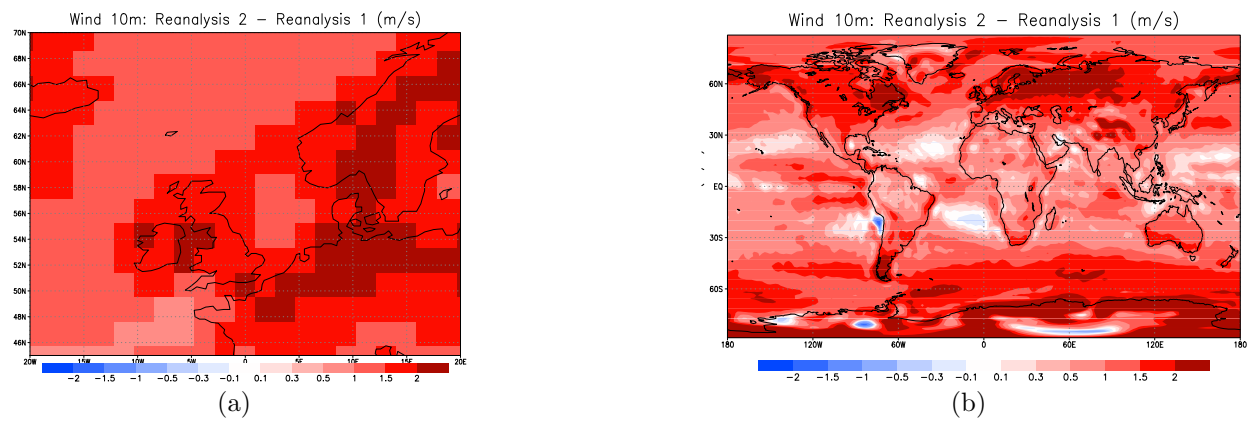


FIG. 7. Bias between the 10 m forecast wind speed of the NRA\_R2 and NRA\_R1 in the eastern North Atlantic and the North Sea (left) and globally (right) in 1998 .

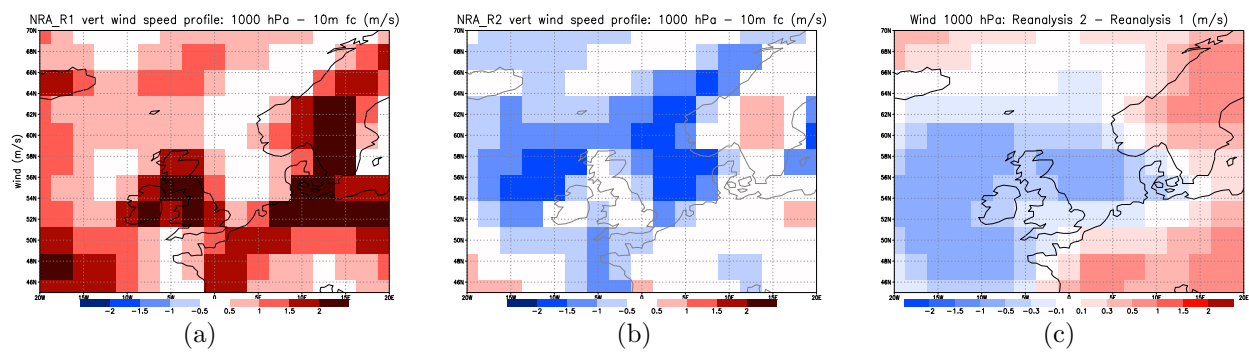


FIG. 8. Comparison of the reanalysed 1000 hPa and forecast (fc) 10 m wind speed of both reanalyses in 1998: a) NRA\_R1: 1000 hPa - 10 m fc, b) NRA\_R2: 1000 hPa - 10 m fc, c) 1000 hPa: NRA\_R2 - NRA\_R1.

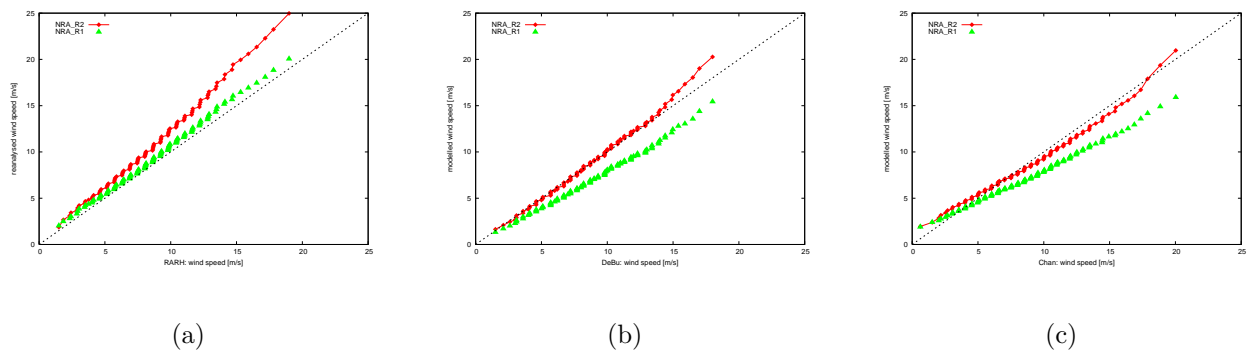


FIG. 9. Comparison of percentile-percentile distributions of 10 m wind speed from NRA\_R1 and NRA\_R2 forecasts (y-axis) and in-situ data (x-axis) at a) the buoy RARH as an open ocean station and b) the light ships DeBu and c) Channel as coastal stations.

# List of Tables

1	Seasonal Brier Skill Scores after Equation 1 using buoy winds as “truth”, NRA_R1 as reference “forecast” and SN-REMO as “forecast”. The buoy winds at K1 and Ems were converted either to the 10m equivalent neutral wind (EQNW) after Liu and Tang (1996) or to the stability dependent wind (STDW) according to the bulk-flux algorithm after Fairall et al. (2003) prior to the BSS calculation. . . . .	44
---	---	----

TABLE 1. Seasonal Brier Skill Scores after Equation 1 using buoy winds as “truth“, NRA\_R1 as reference “forecast“ and SN-REMO as “forecast“. The buoy winds at K1 and Ems were converted either to the 10m equivalent neutral wind (EQNW) after Liu and Tang (1996) or to the stability dependent wind (STDW) according to the bulk-flux algorithm after Fairall et al. (2003) prior to the BSS calculation.

	conv algorithm	BSS			
buoy	STDW/EQNW	DJF	MAM	JJA	SON
K1	EQNW	-0.21	-0.03	-0.08	-0.13
K1	STDW	-0.20	-0.02	-0.08	-0.13
Ems	EQNW	-0.28	-0.30	-0.15	-0.11
Ems	STDW	-0.36	-0.28	-0.10	-0.19